Cancer Research

The Endogenous Tryptophan Metabolite and NAD^+ Precursor Quinolinic Acid Confers Resistance of Gliomas to Oxidative Stress

Felix Sahm[1,2,3], Iris Oezen[1,3,4], Christiane A. Opitz[1,3,4], Bernhard Radlwimmer[5], Andreas von Deimling[2], Tilman Ahrendt[6], Seray Adams[7], Helge B. Bode[6], Gilles J. Guillemin[7], Wolfgang Wick[3,4], and Michael Platten[1,3,4]

Abstract

Quinolinic acid is a product of tryptophan degradation and may serve as a precursor for NAD^+, an important enzymatic cofactor for enzymes such as the DNA repair protein PARP. Pathologic accumulation of quinolinic acid has been found in neurodegenerative disorders including Alzheimer and Huntington disease, where it is thought to be toxic for neurons by activating the N-methyl-D-aspartate (NMDA) receptor and inducing excitotoxicity. Although many tumors including gliomas constitutively catabolize tryptophan, it is unclear whether quinolinic acid is produced in gliomas and whether it is involved in tumor progression. Here, we show that quinolinic acid accumulated in human gliomas and was associated with a malignant phenotype. Quinolinic acid was produced by microglial cells, as expression of the quinolinic acid-producing enzyme 3-hydroxyanthranilate oxygenase (3-HAO) was confined to microglia in glioma tissue. Human malignant glioma cells, but not nonneoplastic astrocytes, expressed quinolinic acid phosphoribosyltransferase (QPRT) to use quinolinic acid for NAD^+ synthesis and prevent apoptosis when *de novo* NAD^+ synthesis was blocked. Oxidative stress, temozolomide, and irradiation induced QPRT in glioma cells. QPRT expression increased with malignancy. In recurrent glioblastomas after radiochemotherapy, *QPRT* expression was associated with a poor prognosis in two independent datasets. Our data indicate that neoplastic transformation in astrocytes is associated with a QPRT-mediated switch in NAD^+ metabolism by exploiting microglia-derived quinolinic acid as an alternative source of replenishing intracellular NAD^+ pools. The elevated levels of QPRT expression increase resistance to oxidative stress induced by radiochemotherapy, conferring a poorer prognosis. These findings have implications for therapeutic approaches inducing intracellular NAD^+ depletion, such as alkylating agents or direct NAD^+ synthesis inhibitors, and identify QPRT as a potential therapeutic target in malignant gliomas. *Cancer Res; 73(11); 3225–34. ©2013 AACR.*

Introduction

Constitutive catabolism of trp has been observed in various types of cancers where it contributes to the suppression of antitumor responses (1). Thus, this trp pathway driven by the rate-limiting enzyme, indoleamine-2,3-dioxygenase (IDO-1), has evolved as a therapeutic target in cancer-associated immunosuppression and both cancer- and autoimmune-mediated inflammation (2–6). Inhibitors of IDO-1 have already entered clinical trials (7, 8). Others and we recently showed that tryptophan-2,3-dioxygenase (TDO), which has previously been described as liver and neuron specific, is expressed in certain cancers (9) such as gliomas and constitutively generates kynurenine (kyn). Glioma cell-derived kyn promotes tumor cell survival, motility, and immune escape (10). Conversely, pharmacologic inhibition of TDO enhances the efficacy of cancer vaccination in preclinical models (11). Although kyn accumulates in glioma cell cultures, the downstream kyn catabolite quinolinic acid was detectable in human glioma tissue (10) indicating that trp is further catabolized in gliomas *in situ*, possibly by infiltrating monocytic cells, which display the enzymatic ability to convert trp and/or kyn to quinolinic acid (12). Quinolinic acid accumulates in neurodegenerative and inflammatory central nervous system (CNS) diseases and has chiefly been studied as an endogenous ligand of the N-methyl-D-aspartate (NMDA) receptor (13, 14) where it induces neuronal loss through excitotoxicity (15). In contrast, monocytic cells,

Authors' Affiliations: [1]Clinical Cooperation Unit Neuroimmunology and Brain Tumor Immunology, German Cancer Research Center (DKFZ); Departments of [2]Neuropathology and [3]Neurooncology, University Hospital Heidelberg; [4]National Center for Tumor Diseases; [5]Division of Molecular Genetics, German Cancer Research Center (DKFZ), Heidelberg; [6]Merck Stiftungsprofessur für Molekulare Biotechnologie, Fachbereich Biowissenschaften, Goethe Universität, Frankfurt, Germany; and [7]Australian School of Advanced Medicine, Macquarie University, North Ryde, New South Wales, Australia

Note: Supplementary data for this article are available at Cancer Research Online (http://cancerres.aacrjournals.org/).

Corresponding Author: Michael Platten, Department of Neurooncology, University Hospital Heidelberg, INF 400, 69120 Heidelberg, Germany. Phone: 49-6221-56-6804; Fax: 49-6221-56-7554; E-mail: michael.platten@med.uni-heidelberg.de

doi: 10.1158/0008-5472.CAN-12-3831

such as macrophages and microglia, induced to catabolize trp convert quinolinic acid to NAD^+ (12).

The capability to prevent hypoxia- or DNA damage-induced cell death despite high proliferative activity is a crucial characteristic of cancer cells (16). NAD^+ plays a key role as a substrate and cofactor maintaining cellular integrity under these conditions. In cancer cells, NAD^+ is depleted by insufficient NAD^+synthesis and NAD^+ consumption by PARP-mediated DNA repair or under hypoxic conditions (17). Therefore, deprivation of NAD^+ has evolved as a target in tumor cell-specific experimental therapies (18). For instance, pharmaceutical targeting of the *de novo* NAD^+ synthesis pathway by FK866, an inhibitor of the nicotinamide phosphoribosyltransferase (NAMPT), sensitizes tumor cells for apoptosis and is currently being evaluated in phase II clinical trials in patients with cancer (19–21). Although the results of therapeutic NAD^+ depletion are promising, the effect of inhibiting NAMPT may be compromised by the activity of quinolinic acid- and nicotinic acid-dependent NAD^+synthesis pathways. Both quinolinic acid and nicotinic acid can serve as alternative substrates for NAD^+ synthesis (22).

As induction of oxidative stress and consecutive NAD^+ depletion are major effects of irradiation and alkylating agents such as temozolomide, we set out to investigate the role of quinolinic acid and the key enzyme for quinolinic acid usage, quinolinic acid phosphoribosyltransferase (QPRT), in human glioma under oxidative stress induced by irradiation and the alkylating agent temozolomide and to delineate the role of this pathway in the resistance to these therapeutic approaches, which constitutes a major problem in the therapy of these tumors.

Materials and Methods

Cell culture and reagents

A172, LN-18, U87MG, LN-229, T98G, and LN-319 human glioma cells and CRL-8621 human astrocytes were purchased from American Type Culture Collection (ATCC; distributed by LGC Standards) between 2007 and 2012. In addition to the tandem repeat analyses at ATCC, cells were tested by multiplex human cell authentication as part of a routine procedure in the German Cancer Research Center (Heidelberg, Germany). The last test was conducted in 2011. Human microglial cells were purchased from Clonexpress. All glioma cells and astrocytes were cultured in Dulbecco's modified Eagle medium (DMEM; Invitrogen), and microglia was incubated in DMEM:F12 (Invitrogen), each supplemented with 10% FBS and 1% penicillin/streptomycin (Sigma-Aldrich). Quinolinic acid (Santa Cruz Biotechnology), FK866 (Axon Medchem), and nicotinic acid (Sigma-Aldrich) were dissolved in dimethyl sulfoxide (Roth). A172 shQPRT cells were generated by transfection with the Origene shQPRT vector (Origene). T325 glioma-initiating cells were generated as described previously (23). HA1800 primary astrocytes were obtained from ScienCell.

Western blot analysis

Twenty micrograms of protein diluted in NuPAGE sample buffer and reducing reagent (Invitrogen) were denatured at 95°C for 5 minutes and electrophoretically separated on ready-to-use 4% to 12% SDS-polyacrylamide gels (Invitrogen). Proteins were blotted onto nitrocellulose membranes (Invitrogen) at 1.5 mA/cm^2 for 1.5 hour. After blocking in 0.5 mol/L Tris–Base, pH 7.4, 5% milk powder, 1.5 mol/L NaCl, 0.05% Tween 20, the membranes were incubated with anti-3-HAO (1:300; Abnova), anti-QPRT (1:500; Sigma-Aldrich), anti-PARP (1:300; Cell Signaling), anti-cleaved PARP (1:300; Cell Signaling), anti-caspase-3 (1:200; Cell Signaling), anti-cleaved caspase-3 (1:200; Cell Signaling), or anti-survivin (Cell Signaling) antibody overnight at 4°C. Staining with anti-rabbit or anti-mouse secondary horseradish peroxidase-conjugated antibodies at dilutions of 1:4,000 (both Cell Signaling), was followed by immunodetection with LumiGLO Chemiluminescent Substrate (KBL).

NAD^+ quantification

Intracellular NAD^+ and NADH levels were measured using the NAD^+/NAD^+H Assay Kit (Abcam) according to the manufacturer's instructions. Briefly, 250,000 cells were seeded and harvested at the endpoint of the respective experiment. Pellets were washed with cold PBS. Then, cells were extracted with NADH/NAD^+ Extraction Buffer by 2 freeze/thaw cycles (20 minutes on dry ice, then 10 minutes at room temperature). Total NAD^+ and NADH were detected following the instructions in a 96-well plate. Color reaction was read with a 450 nm filter (BMG Omega reader; BMG Labtech).

Quinolinic acid quantification

Gas chromatography/mass spectroscopy (GC/MS) was conducted to determine the levels of quinolinic acid and picolinic acid in the supernatant of growing cells in culture. The GC/MS method used for the analysis of picolinic acid and quinolinic acid has been described previously (24). Briefly, the internal standards used were picolinic acid conjugated with deuterium D4 picolinic acid and quinolinic acid conjugated with deuterium D3 quinolinic acid (Medical Isotopes). Protein in culture supernatants was precipitated by the addition of an equal volume of 10% trichloracetic acid (Sigma-Aldrich; 1:1) and centrifuged at 1,000 rpm for 5 minutes. For the derivatization procedure, standards and sample solutions (100 μL) were then transferred to glass tissue culture vials (100 × 10 mm) with the addition of 10 μL picolinic acid and 10 μL quinolinic acid internal standards and then evaporated to dryness using the SpeedVac. A total of 60 μL of trifluoroacetic anhydride (Sigma-Aldrich) and 60 μL of 1,1,1,3,3,3-hexafluoro-2-propanol were then added to the residues. The glass vials were then capped and sealed immediately and heated at 60°C for 30 minutes to produce the hexafluoroisopropyl ester of the respective acids. The ester products were then dissolved in 180 μL of toluene, washed with 5% sodium bicarbonate (1 mL) and water (1 mL), dried over anhydrous sodium sulfate (~500 mg), and transferred to autosampler vials before injection (1 μL) into the GC/MS via 7683 Autosampler (Agilent). Standard solutions of quinolinic acid and picolinic acid for calibration curves were prepared from stock solutions. The final concentrations of unknowns were calculated by interpolation of the standard curves.

Cell viability assay

Cell viability was assessed using crystal violet staining or the MTT assay. For crystal violet staining, cells were fixed for 10 minutes in 4% formaldehyde, rinsed twice with PBS (Invitrogen), and dried. Cells were stained with 0.1% crystal violet solution for 30 minutes. Excess stain was washed out applying once PBS and twice distilled water. Plates were dried again. The crystal violet was dissolved in 100 μL of 10% acetic acid solution per well. Plates were read in a plate reader (BMG Omega) with a 560 nm filter. The MTT assay was conducted using standard conditions. In brief, cells were incubated with MTT for 3.5 hours at 37°C followed by incubation with MTT solvent for 15 minutes at room temperature. Absorbance was read at 590 nm.

Quantitative real-time PCR

Total RNA was isolated with the NucleoSpin RNA II Extraction Kit (Macherey Nagel) and cDNA was synthesized with the Quantitect Reverse Transcription Kit (Qiagen) according to manufacturer's instructions. Quantitative real-time PCR (qRT-PCR) was conducted with Quantitect Primers for *QPRT* or glyceraldehyde-3-phosphate dehydrogenase (*GAPDH*; Qiagen) in an ABI 7300 thermal cycler (Applied Biosystems) with Quantifast SYBR Green PCR Kit (Qiagen) according to standard protocols. PCRs were checked by including no-RT controls, by omission of templates and by both melting curves. Standard curves were generated for each gene. Relative quantification of gene expression was determined by comparison of threshold values, normalized to *GAPDH*, calculated by 2 $(-\Delta\Delta C_t)$. Primers for *QPRT*, 3-hydroxyanthranilate oxygenase (*3-HAO*), and *GAPDH* were obtained from Qiagen.

Human tissue samples and immunohistochemistry

Sixty formalin-fixed paraffin-embedded glioma tissue samples and 2 cortex control tissues were obtained from the Department of Neuropathology, Institute of Pathology, (Heidelberg, Germany) banked in the Department of Neuropathology, and administered by the tissue bank of the German National Center for tumor diseases (Heidelberg, Germany) tissue bank. Tissue analyses were approved by local and national authorities. Sections cut to 3 μm were incubated and processed with anti-QPRT, anti-3-HAO, anti-CD68, antiquinolinic acid (1:25; Abcam), or anti-GFAP (Dako) on a VentanaBenchMark XT immunostainer (Ventana Medical Systems). The Ventana staining procedure included pretreatment with cell conditioner 2 (pH 6) for 60 minutes, followed by incubation with the primary at 37°C for 32 minutes. Incubation was followed by Ventana standard signal amplification, UltraWash, counterstaining with one drop of hematoxylin for 4 minutes and one drop of bluing reagent for 4 minutes. For visualization, ultraViewUniversal DAB Detection Kit (Ventana Medical Systems) was used. QPRT expression was scored according to the H-Score described by Bruna and colleagues (25). Quinolinic acid staining patterns were quantified by dividing staining intensity into 4 subgroups: strong (3), intermediate (2), weak (1), or absent (0), multiplied by 2 if > 10 positive foci in 4 high-power magnification fields (× 400) were detectable. For immunofluorescence, sections cut to 3 μm were pretreated for 30 minutes in cell conditioner 1 (Ventana) incubated with anti-QPRT (1:100), anti-CX3CR1 (Santa-Cruz; 1:50), anti-3-HAO (1:500), antiquinolinic acid (1:100), and anti-CD68 (1:50; Dako) antibodies for 2 hours at room temperature. Secondary antibodies anti-mouse and anti-rabbit (1:500, all Alexafluor488 or Alexafluor568, respectively; Invitrogen) were applied for 30 minutes at room temperature.

Statistical analysis

Statistical analysis was conducted using Microsoft Excel 2003 (Microsoft) or provided directly by the analysis tools of the expression data platforms. Student *t* test (2 tailed) was applied for analyses of 2 subsets or one-way ANOVA of larger series. Survival data were analyzed by log-rank tests. *P* values < 0.03 were considered significant, whereas $P < 0.01$ were highly significant. Immunoblot quantification was conducted applying ImageJ version 1.44 (rsbweb.nih.gov). Statistical testing of gene expression data obtained from the R2 platform (http://hgserver1.amc.nl/) was conducted using the included online tool.

Results

TDO-derived quinolinic acid accumulates in glioma

We first analyzed the degree of quinolinic acid accumulation in glioma tissue. Immunohistochemistry revealed strong accumulation of quinolinic acid in glioma tissue, whereas normal cortex was devoid of quinolinic acid-positive cells (Fig. 1A).

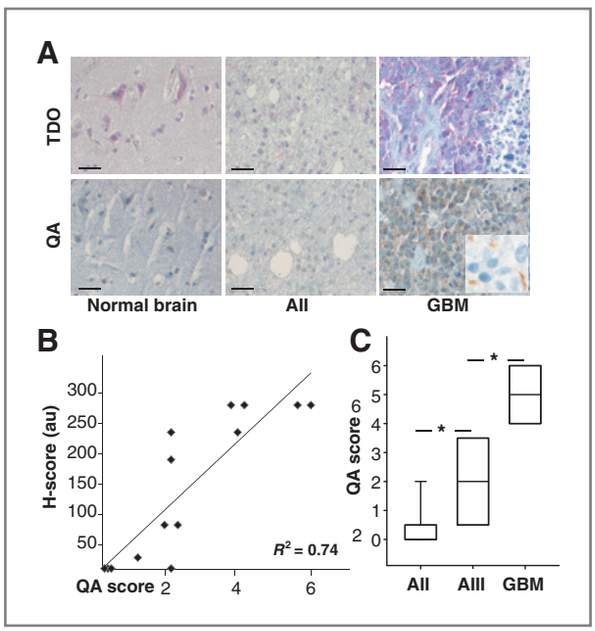

Figure 1. A, photomicrographs of the immunohistochemical detection of TDO (top row) and quinolinic acid (QA; bottom row) in control cortex (left), astrocytoma grade II (middle), and glioblastoma (GBM; right). Bar, 25 μm. B, quantification of TDO expression using H-score plotted against the quinolinic acid score in glioma sections ($n = 14$); $r^2 = 0.74$. C, quinolinic acid accumulation in tumor tissue of astrocytic tumors of WHO II, III, and IV as determined by the quinolinic acid score. *, $P = 0.004$ (AII–AIII) and $P = 0.003$ (AIII–GBM); $n = 14$.

High levels of quinolinic acid in gliomas correlated with the expression of TDO (Fig. 1A and B) and were associated with a malignant phenotype (Fig. 1A and C). These data indicated that TDO-mediated trp catabolism not only promotes kyn accumulation (10) but also accumulation of quinolinic acid in glioma tissue. As described previously (10), IDO-1 expression in malignant gliomas was confined to infiltrating leukocytes and endothelial cells but largely absent in tumor cells (Supplementary Fig. S1E).

Quinolinic acid constitutes a NAD^+ salvage pathway in gliomas and protects from stress-induced apoptosis

As quinolinic acid may serve as a precursor for NAD^+ (22), which in turn may protect tumor cells from oxidative stress (17), we next assessed the functional consequences of quinolinic acid for NAD^+-mediated cytoprotection in malignant gliomas. Blocking the *de novo* NAD^+ synthesis using the NAMPT-inhibitor, FK866, significantly reduced NAD^+ levels in glioma cells and in nonneoplastic astrocytes (Supplementary Fig. S3A). Viability of astrocytes but not glioma cells was reduced by NAMPT inhibition alone, whereas FK866 treatment strongly reduced cell viability in both astrocytes and glioma cells subjected to oxidative stress induced by subtoxic concentrations of hydrogen peroxide (H_2O_2; Fig. 2A and B), indicating that both astrocytes and glioma cells require NAMPT-mediated NAD^+ synthesis for the protection from oxidative stress. Quinolinic acid restored cell viability induced by combined oxidative stress and NAMPT inhibition in glioma cells (Fig. 2A and Supplementary Fig. S2A) but not in astrocytes (Fig. 2B and Supplementary Fig. S2B), indicating that glioma cells specifically used quinolinic acid to replenish NAD^+ stocks. In fact, NAD^+ levels in FK866-treated A172 cells increased by addition of quinolinic acid (Supplementary Fig. S3C). Conversely, nicotinic acid restored cell viability in stressed and NAD^+-depleted astrocytes but not in glioma cells (Fig. 2A and B and Supplementary Fig. S2). These data indicate that the quinolinic acid-fed but not the nicotinic acid-fed NAD^+ salvage pathway is active in gliomas, whereas astrocytes use the nicotinic acid-fed rather than the quinolinic acid-fed salvage pathway to protect themselves from the functional consequences of oxidative stress in conditions of reduced NAD^+ availability. Quinolinic acid-mediated rescue of cell viability in gliomas was associated with suppression of apoptosis as evidenced by cleavage of PARP and caspase-3 and reduction of survivin (Fig. 2C). Collectively, these data suggest that malignant transformation of astrocytes is associated with a switch from the nicotinic acid salvage pathway to the quinolinic acid salvage pathway to synthesize NAD^+ to protect glioma cells from cell death induced by oxidative stress and NAD^+ depletion. To address the effect of quinolinic acid in response to current therapeutic settings, we analyzed the effect of quinolinic acid supplementation to cells treated with

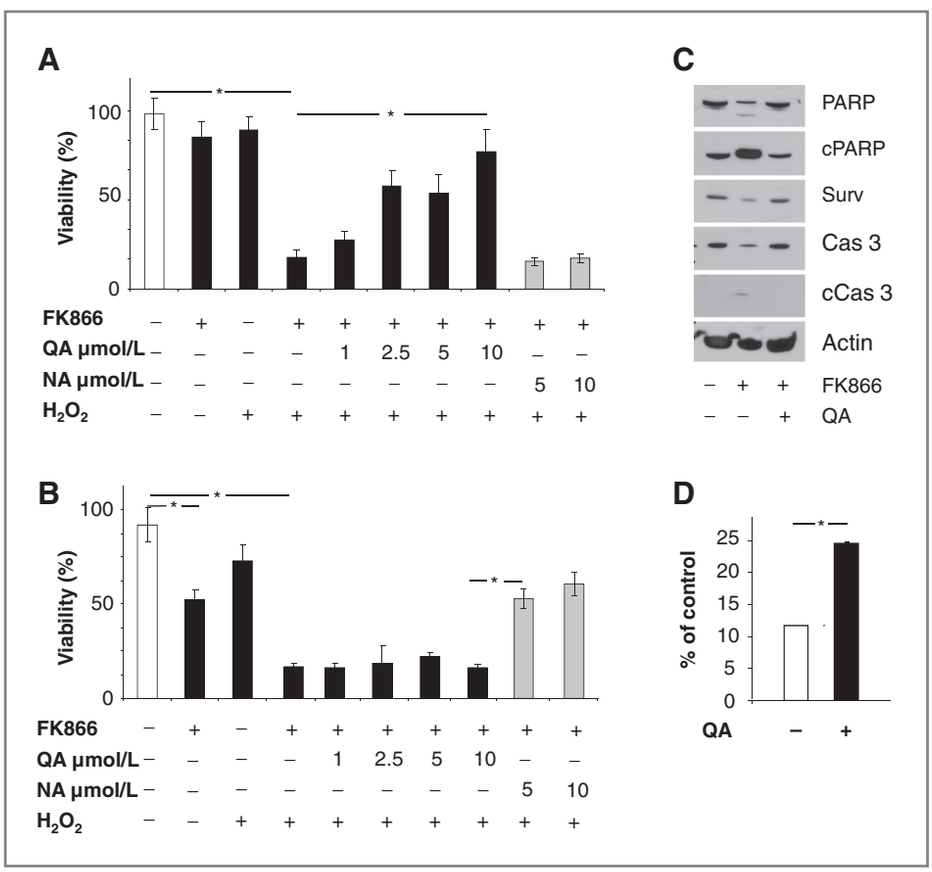

Figure 2. A, viability of glioma cells under oxidative stress, NAD^+ depletion, and substitution of either quinolinic acid (QA) or nicotinic acid (NA), 10 to 0 µmol/L quinolinic acid (*, $P < 0.0001$), FK866+H_2O_2 – control (*, $P = 0.001$). B, viability of astrocytes under oxidative stress, NAD^+ depletion, and substitution of either quinolinic acid or nicotinic acid, 5 to 0 µmol/L nicotinic acid (*, $P < 0.0001$), FK866 + H_2O_2 – control (*, $P = 0.0002$), FK866 – control (*, $P = 0.01$). C, detection of markers for apoptosis in A172 glioma cells treated with FK866 with and without quinolinic acid (c, cleaved; Surv, survivin; Cas 3, caspase-3). D, viability of A172 glioma cells treated with FK866 and the alkylating agent temozolomide instead of H_2O_2 to induce oxidative stress, substituted with quinolinic acid (*, $P = 0.003$).

temozolomide. Temozolomide treatment reduced intracellular NAD^+ levels in (Supplementary Fig. S1B) and viability of glioma cells (Fig. 2D). Quinolinic acid restored viability of cells treated with temozolomide and FK866 (Fig. 2D), indicating that quinolinic acid accumulation in gliomas leads to resistance to alkylating chemotherapy in NAD^+-depleted conditions.

QPRT is expressed in malignant gliomas and responsible for NAD^+ synthesis

To identify the enzymatic requirements for quinolinic acid-mediated protection of glioma cells, we analyzed the expression of QPRT, the enzyme that is responsible for the generation of NAD^+ from quinolinic acid. Glioma cells express high levels of QPRT, whereas it is virtually absent in astrocytes. In contrast, astrocytes show high expression of nicotinic acid phosphoribosyltransferase (NAPRT), whereas it is low to absent in glioma cells (Fig. 3A). These differences in the expression of NAD^+ salvage pathway enzymes may explain why glioma cells use the quinolinic acid pathway, whereas nonneoplastic astrocytes rely on the nicotinic acid pathway. To characterize QPRT expression *in vivo*, we analyzed human glioma tissue. QPRT was weakly expressed in low-grade gliomas, whereas gliomas of higher malignancy exhibited strong expression as detected by immunohistochemistry (Fig. 3B and E). In line with the virtually exclusive expression of NAPRT in nonneoplastic astrocytes *in vitro*, staining of NAPRT was confined to reactive astrocytes in glioma tissue and not observed in tumor cells (Fig. 3C). Analysis of expression data of World Health Organization (WHO) grade 2–4 glioma from the German Brain Tumor Network (26) yielded higher levels of *QPRT* with increasing malignancy (Fig. 3D). Moreover, Western blot analysis showed higher QPRT expression in glioblastoma than in low-grade glioma samples (Fig. 3F). Of note, no upregulation of expression with malignancy was seen for *NAPRT* confirming the immunohistochemistry data, which show that NAPRT is confined to nonneoplastic tissue (ref. 27; Supplementary Fig. S4).

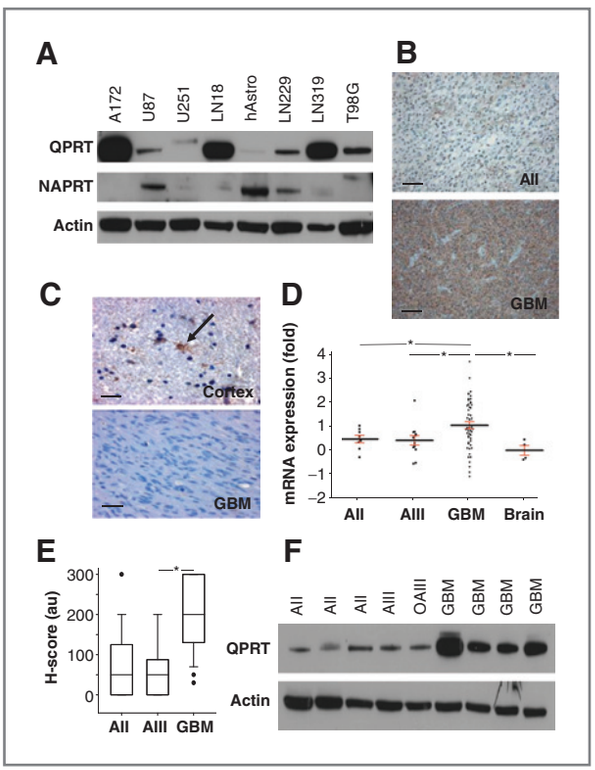

Figure 3. A, expression of QPRT and NAPRT in malignant glioma cell lines A172, U87MG, U251, LN18, LN229, LN319, T98G, and human astrocytes, with actin as loading control. B, immunohistochemistry for QPRT in glioblastoma (GBM) and astrocytoma grade 2 (AII), with cortex tissue as control. Bar, 100 μm. C, immunohistochemistry for NAPRT in glioblastoma tissue (bottom panel) and adjacent reactive tissue. Arrow, reactive astrocyte. Bar, 25 μm. D, expression data of *QPRT* retrieved from a dataset of grade 2–4 astrocytoma tissue lysates (26); *, $P = 0.0263$ ($n = 74$). E, score of QPRT expression detected by immunohistochemistry in diffuse glioma WHO grade 2–4, AIII – GBM; *, $P = 0.018$ ($n = 49$). F, expression as detected by immunoblot analysis of QPRT in diffuse glioma.

QPRT protects glioma cells from oxidative stress and confers an unfavorable prognosis

Our results indicate that QPRT expression is involved in protecting gliomas from oxidative stress induced by alkylating agents. Thus, we evaluated whether cytoprotective QPRT is upregulated by gliomas cells in response to oxidative stress measures. Expression analyses by qRT-PCR showed that temozolomide, irradiation, and H_2O_2 treatment dose dependently induced the expression of *QPRT* (Fig. 4A). To assess this effect on the protein level *in vivo*, we analyzed matched pairs of tumor tissue resected before and after radiochemotherapy. Tumor tissue resected after radiochemotherapy showed higher expression of QPRT compared with samples before treatment (Fig. 4B; for patient characteristics see Supplementary Table S1). To analyze the functional consequences of QPRT in gliomas, we generated stable knockdown cells using short hairpin RNA (Supplementary Fig. S5A). Silencing of *QPRT* abrogated the protective effects of quinolinic acid from NAD^+ depletion in gliomas cells (Fig. 4C). Biostatistical testing for correlation between *QPRT* expression and survival based on REpository for Molecular BRAin Neoplasia DaTa (REMBRANDT; rembrandt.nci.nih.gov) showed that high *QPRT* expression in gliomas tissue is associated with an unfavorable prognosis (Fig. 4D). Moreover, *QPRT* expression also stratifies for survival within the subgroup of patients with glioblastoma in an independent dataset (ref. 28; Supplementary Fig. S6). Collectively these data indicate that in gliomas, QPRT is upregulated in response to oxidative stress imposed by radiochemotherapy to protect glioma cells from these therapeutic measures by activating an NAD^+ salvage pathway that is distinct from nonneoplastic astrocytes.

Quinolinic acid in human gliomas is provided by infiltrating microglial cells

To determine whether glioma cells are capable of producing quinolinic acid, we analyzed the cell culture supernatant for

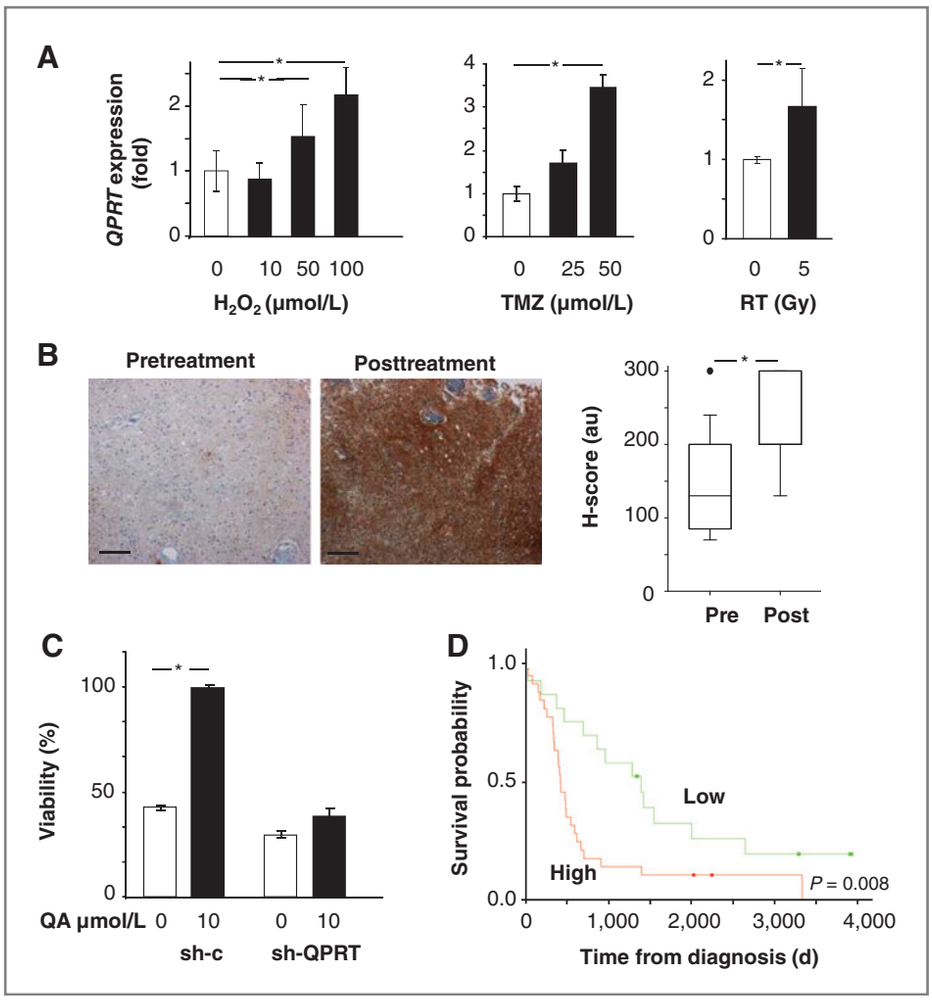

Figure 4. A, qRT-PCR for *QPRT* in A172 glioma cells treated with H_2O_2 (50 μmol/L: *, $P = 0.017$; 100 μmol/L: *, $P = 0.008$), temozolomide (TMZ) (*, $P = 0.003$), or radiation (RT; *, $P < 0.001$). B, immunohistochemical detection of QPRT in matched tissue samples resected before and after radiochemotherpy (RCtx); *, $P = 0.018$. Bar, 100 μm ($n = 11$). C, viability of shQPRT A172 glioma cells treated with FK866 and substituted with quinolinic acid (QA), controls; *, $P = 0.005$. D, survival data retrieved from Rembrandt for patients with glioma suffering tumors with high or low *QPRT* expression.

the presence of quinolinic acid using GC/MS (24). We used glioma cells, which we have previously shown to catabolize trp constitutively through the enzymatic activity of TDO (10). Quinolinic acid is converted from the kyn metabolite 3-hydroxyanthranilate by 3-HAO (27). All but one trp-catabolizing glioma cell line lacked 3-HAO expression explaining the inability of these cells to generate quinolinic acid (Fig. 5A). However, Western blot analyses of glioma tissue revealed strong expression of 3-HAO in glioblastoma, but not in low-grade glioma tissues (Fig. 5B). Glioblastomas are frequently infiltrated by high numbers of microglial cells, which may account for almost 50% of the total cellular mass in these tumors and may promote rather than inhibit tumor growth by various mechanisms (29). Microglial cells have been shown to be capable of generating quinolinic acid (30, 31). In line, microglia supernatant showed the highest levels of quinolinic acid compared with glioma cells and astrocytes (Supplementary Fig. S7). Indeed, immunohistochemistry showed that 3-HAO is strongly expressed in cells that also express the microglia marker CD68 (Fig. 5C). Immunofluorescent double labeling confirmed coexpression of the microglia markers CD68 or CX3CR1, respectively, and 3-HAO and colocalization of $CD68^+$ and quinolinic acid in glioma tissue (Fig. 5D and Supplementary Fig. S5B). To analyze the influence of quinolinic acid-producing microglial cells, we used primary human cultured microglia capable of generating quinolinic acid (Supplementary Fig. S7). Quinolinic acid-containing microglial supernatant increased viability of QPRT-proficient but not QPRT-deficient glioma cells in a NAD^+-depleted condition (Fig. 5E). These data indicate that microglial cells contribute to the resistance of gliomas to oxidative stress induced by radiochemotherapy by converting glioma-derived kyn to quinolinic acid, which in turn is used by gliomas cells to replenish depleted intracellular NAD^+ pools (Fig. 6).

Discussion

Resistance toward radiochemotherapy constitutes a major problem in the therapy of malignant gliomas. Although irradiation plus concomitant and adjuvant chemotherapy with temozolomide represents the standard of care for patients with glioblastoma (32), resistance to these therapies is encountered during primary therapy, particularly in elderly patients (33), or in the recurrent setting despite considerable efforts to intensify chemotherapeutic regimens with the aim at overcoming

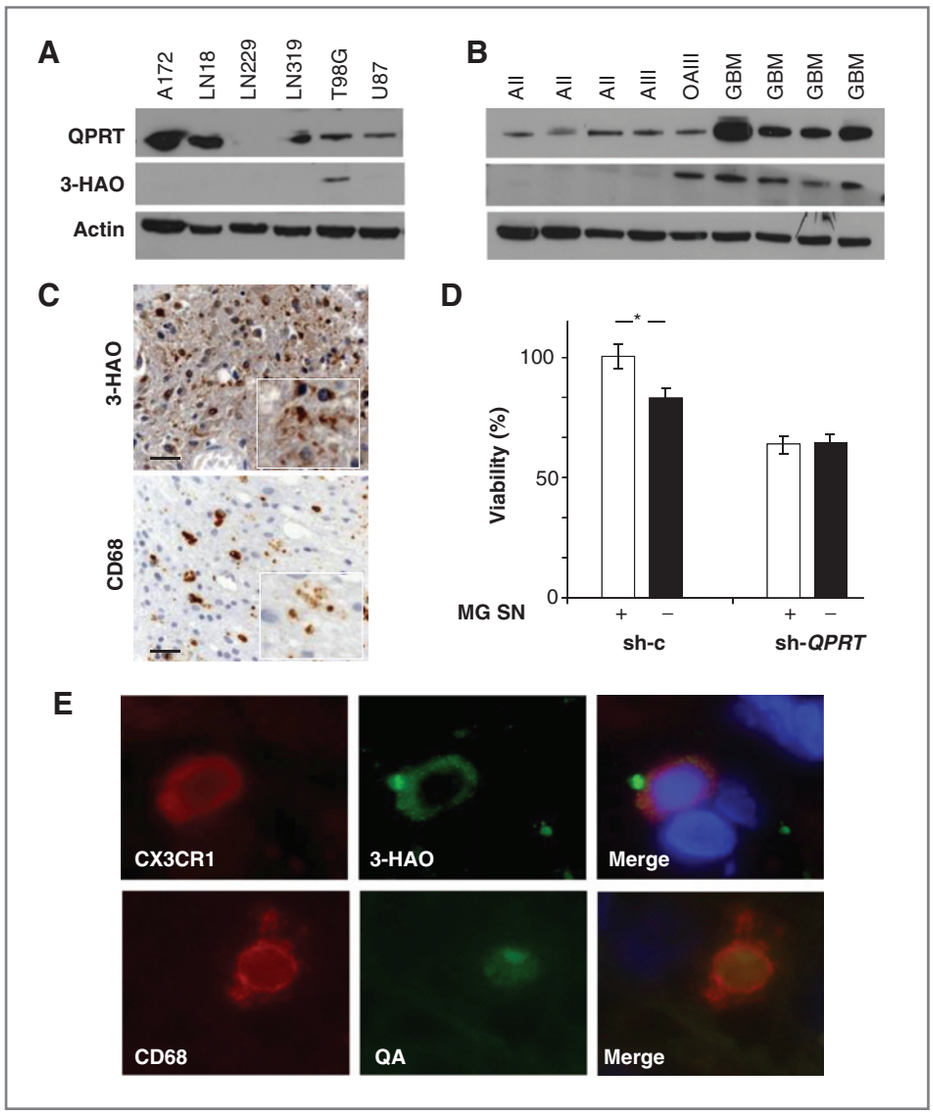

Figure 5. Immunoblot analyses for QPRT and 3-HAO expression in glioma cell lines, actin as control (A) and glioma tissue lysates (B). C, immunohistochemistry for 3-HAO and CD68 in glioma tissue. Bar, 25 μm. D, viability of shQPRT and control (sh-c) cells treated with FK866 and supplemented with microglia supernatant (MG SN); *, $P = 0.02$. E, immunofluorescent localization of CX3CR1, 3-HAO, quinolinic acid (QA), and CD68 in glioma tissue.

primary or secondary resistance (34). Although the activities of methyltransferases, particularly MGMT, have evolved as major factors predicting response to alkylating agents in the primary setting (35), the factors, which are induced by primary therapeutic measures and constitute resistance in the recurrent setting beyond functional alterations in DNA mismatch repair capabilities (36), are incompletely understood. We provide here, evidence for a novel therapeutic pathway, which confers resistance of malignant gliomas to radiochemotherapy involving the synthesis of NAD^+ from quinolinic acid via QPRT, an enzyme that is induced in recurrent malignant gliomas and associated with poor prognosis in these tumors (Figs. 3B and 4D and Supplementary Fig. S6). The main finding of this study is that microglial 3-HAO activity in gliomas is capable of providing the NAD^+ precursor quinolinic acid, which confers resistance to oxidative stress as invoked by, for instance, irradiation or temozolomide. These results suggest that microglial cells contribute to the chemo- and radio-resistant phenotype of gliomas. Previous studies reported correlation of microglial invasion with aggressiveness and poor prognosis in gliomas by releasing growth promoting, angiogenic, and immunosuppressive factors (37–40). Our results suggest that infiltrating microglial cells may shape the tumor microenvironment to not only negatively influence the natural course of disease but also the response to therapy. The mechanism involved in this host-mediated resistance pathway involves the catabolism of the essential amino acid trp. Trp metabolism has thus far chiefly been viewed as a metabolic pathway used by various types of cancer to suppress antitumor immune responses (18). A measure of catabolic activity of cancer-derived IDO-1 or TDO has consistently been the depletion of trp and the accumulation of kyn, both of which, through the activation of amino acid starvation and receptor-mediated pathways, respectively, result in suppression of T-cell responses (10, 41). However, it has long been known that metabolites further downstream of kyn, such as kynurenic

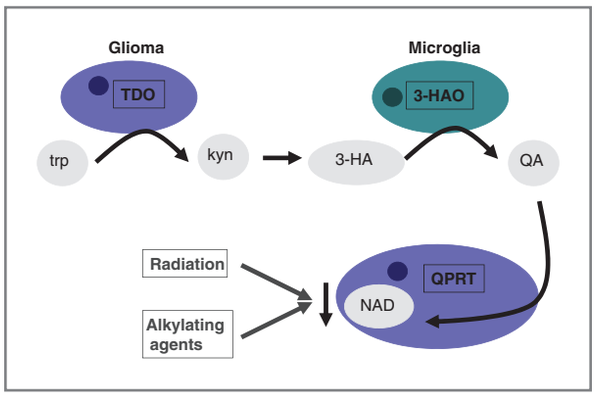

Figure 6. Scheme of interaction between microglia and glioma cells in degradation of tryptophan and usage of quinolinic acid. QA, quinolinic acid; trp, tryptophan; kyn, kynurenine; 3-HA, 3-hydroxy-anthrananilic acid; TDO, tryptophan-2,3-dioxygenase; 3-HAO, 3-hydroxy-anthranilic acid oxygenase; QPRT, quinolinic acid phosphoribosyl transferase; NAD, nicotinamide adenine dinucleotide.

acid, 3-hydroxy-kynurenine, and 3-hydroxy-anthranilic acid, may suppress T-cell immunity (6, 42, 43). Here, we explored the relevance of trp catabolism in malignant gliomas beyond immunoactive metabolites and addressed the relevance of quinolinic acid for stress resistance. Quinolinic acid has previously mainly been studied as a neurotoxin accumulating in the CNS of patients with neurodegenerative diseases where it causes excitotoxicity by binding and activating the NMDA receptor (44–47). Its physiologic relevance as a NAD^+ precursor has received much less attention possibly because it has been viewed as a less relevant NAD^+ synthesis pathway compared with the *de novo* NAD^+ synthesis pathway through NAMPT or the NAD^+-recycling pathway through NAPRT. However, tryptophan catabolism appears in principle capable of replenishing depleted intracellular NAD^+ stores and protecting cells from oxidative stress as evidenced by *in vitro* studies (48–51). These studies also showed that nicotinic acid is a preferred route of NAD^+ synthesis in murine astrocytes in line with our findings in human cells and tissue (50). Our results indicate the specific capability of glioma cells to use the trp metabolite quinolinic acid as a NAD^+ precursor, whereas nonneoplastic astrocytes use nicotinic acid. Although we did not detect QPRT in 2 independent astrocyte cells, previous studies found strong induction of QPRT and subsequent degradation of quinolinic acid in cultured astrocytes in response to tryptophan metabolites and proinflammatory cytokines (52).

The enrichment of quinolinic acid-metabolizing QPRT in glioma cells (Fig. 3A), its induction by radiochemotherapeutic treatment measures (Fig. 4A and B), and its association with higher malignancy and poor prognosis in gliomas (Figs. 3B and D and 4D) signify its biologic relevance as opposed to the nicotinic acid-metabolizing NARPT, which is confined to reactive astrocytes (Fig. 3C), not associated with malignancy (Supplementary Fig. S4), and not specific for neoplastic glial cells (Fig. 3A). It is tempting to speculate that malignant transformation and therapeutic measures such as radiation therapy and (alkylating) chemotherapy result in nicotinic acid depletion in the tumor microenvironment, which in turn induces a selection pressure for tumor cells capable of using quinolinic acid as an alternative source of NAD^+. Still, this switch relies on the presence of infiltrating microglial cells as a provider of quinolinic acid. Studies in monocytic cells including microglial cells have indicated their capability of accumulating quinolinic acid after induction of IDO-1 by inflammatory mediators (12, 53, 54). Our results indicate that glioma cells themselves are not capable of metabolizing tryptophan to quinolinic acid as they lack the key enzyme 3-HAO (Fig. 5A and B). Hence, local inflammation may create an environment in the tumor, which results in the attraction and activation of quinolinic acid-producing microglial cells, may enable trp-metabolizing tumor cells to defend themselves from oxidative stress. In this respect, the function of microglial cells may be similar to neurodegenerative diseases where quinolinic acid-degrading microglial cells seem to prevent neurotoxicity (55). In addition to suppressing antitumor immune responses and promoting cell survival and cell motility, trp metabolism may thus also constitute a novel metabolic mechanism to confer resistance of tumor cells to radiochemotherapy. This metabolic pathway may explain why NAD^+-depleting agents, such as FK866, are of limited efficacy in some tumors such as malignant gliomas and neuroblastomas, where quinolinic acid has been shown to be proproliferative (56, 57). The resistance mechanism, as suggested by our data, seems to be regulated at the level of QPRT, which is why this enzyme may be a novel therapeutic target in malignant gliomas. Of note, association of high *QPRT* expression and unfavourable clinical course is not limited to glioma but also indicated by expression data from acute myeloid leukemia (58). Although currently available substances, which inhibit QPRT, such as phtalic acid, are unspecific, the rational design of QPRT inhibitors may lead to a novel pharmacologic approach to target resistance of tumors to radiochemotherapy.

Disclosure of Potential Conflicts of Interest

No potential conflicts of interest were disclosed.

Authors' Contributions

Conception and design: W. Wick, M. Platten
Development of methodology: F. Sahm, H.B. Bode, G.J. Guillemin, M. Platten
Acquisition of data (provided animals, acquired and managed patients, provided facilities, etc.): F. Sahm, I. Oezen, A. von Deimling, G.J. Guillemin
Analysis and interpretation of data (e.g., statistical analysis, biostatistics, computational analysis): F. Sahm, I. Oezen, C.A. Opitz, B. Radlwimmer, T. Ahrendt, H.B. Bode, G.J. Guillemin, W. Wick, M. Platten
Writing, review, and/or revision of the manuscript: F. Sahm, I. Oezen, C.A. Opitz, A. von Deimling, S. Adams, G.J. Guillemin, W. Wick, M. Platten
Study supervision: M. Platten

Grant Support

This work was supported by grants from the German Cancer Aid (110392), the German Research Foundation (Deutsche Forschungsgemeinschaft SFB 938 TP K), and the Helmholtz Association (VH-NG-306) to M. Platten and the Hertie Foundation to W. Wick.

The costs of publication of this article were defrayed in part by the payment of page charges. This article must therefore be hereby marked *advertisement* in accordance with 18 U.S.C. Section 1734 solely to indicate this fact.

Received October 3, 2012; revised February 28, 2013; accepted March 2, 2013; published OnlineFirst April 2, 2013.

References

1. Platten M, Wick W, Van den Eynde BJ. Tryptophan catabolism in cancer: beyond IDO and tryptophan depletion. Cancer Res 2012;72:5435–40.
2. Munn DH, Mellor AL. Indoleamine 2,3-dioxygenase and tumor-induced tolerance. J Clin Invest 2007;117:1147–54.
3. Muller AJ, DuHadaway JB, Donover PS, Sutanto-Ward E, Prendergast GC. Inhibition of indoleamine 2,3-dioxygenase, an immunoregulatory target of the cancer suppression gene Bin1, potentiates cancer chemotherapy. Nat Med 2005;11:312–9.
4. Muller AJ, Prendergast GC. Marrying immunotherapy with chemotherapy: why say IDO? Cancer Res 2005;65:8065–8.
5. Prendergast GC, Metz R, Muller AJ. Towards a genetic definition of cancer-associated inflammation: role of the IDO pathway. Am J Pathol 2010;176:2082–7.
6. Platten M, Ho PP, Youssef S, Fontoura P, Garren H, Hur EM, et al. Treatment of autoimmune neuroinflammation with a synthetic tryptophan metabolite. Science 2005;310:850–5.
7. Hou DY, Muller AJ, Sharma MD, DuHadaway J, Banerjee T, Johnson M, et al. Inhibition of indoleamine 2,3-dioxygenase in dendritic cells by stereoisomers of 1-methyl-tryptophan correlates with antitumor responses. Cancer Res 2007;67:792–801.
8. Munn DH. Blocking IDO activity to enhance anti-tumor immunity. Front Biosci 2012;4:734–45.
9. Pilotte L, Larrieu P, Stroobant V, Colau D, Dolusic E, Frederick R, et al. Reversal of tumoral immune resistance by inhibition of tryptophan 2,3-dioxygenase. Proc Natl Acad Sci U S A 2012;109:2497–502.
10. Opitz CA, Litzenburger UM, Sahm F, Ott M, Tritschler I, Trump S, et al. An endogenous tumour-promoting ligand of the human aryl hydrocarbon receptor. Nature 2011;478:197–203.
11. Dolusic E, Larrieu P, Moineaux L, Stroobant V, Pilotte L, Colau D, et al. Tryptophan 2,3-dioxygenase (TDO) inhibitors. 3-(2-(pyridyl)ethenyl) indoles as potential anticancer immunomodulators. J Med Chem 2011;54:5320–34.
12. Guillemin GJ, Smythe G, Takikawa O, Brew BJ. Expression of indoleamine 2,3-dioxygenase and production of quinolinic acid by human microglia, astrocytes, and neurons. Glia 2005;49:15–23.
13. Ting KK, Brew BJ, Guillemin GJ. Effect of quinolinic acid on human astrocytes morphology and functions: implications in Alzheimer's disease. J Neuroinflammation 2009;6:36.
14. Nemeth H, Toldi J, Vecsei L. Kynurenines, Parkinson's disease and other neurodegenerative disorders: preclinical and clinical studies. J Neural Transm Suppl 2006:285–304.
15. Stone TW, Mackay GM, Forrest CM, Clark CJ, Darlington LG. Tryptophan metabolites and brain disorders. Clin Chem Lab Med 2003;41:852–9.
16. Hassa PO. The molecular "Jekyll and Hyde" duality of PARP1 in cell death and cell survival. Front Biosci 2009;14:72–111.
17. Schreiber V, Dantzer F, Ame JC, de Murcia G. Poly(ADP-ribose): novel functions for an old molecule. Nat Rev Mol Cell Biol 2006;7:517–28.
18. Khan JA, Forouhar F, Tao X, Tong L. Nicotinamide adenine dinucleotide metabolism as an attractive target for drug discovery. Expert Opin Ther Tar 2007;11:695–705.
19. Holen K, Saltz LB, Hollywood E, Burk K, Hanauske AR. The pharmacokinetics, toxicities, and biologic effects of FK866, a nicotinamide adenine dinucleotide biosynthesis inhibitor. Invest New Drugs 2008;26:45–51.
20. Hasmann M, Schemainda I. FK866, a highly specific noncompetitive inhibitor of nicotinamide phosphoribosyltransferase, represents a novel mechanism for induction of tumor cell apoptosis. Cancer Res 2003;63:7436–42.
21. Nahimana A, Attinger A, Aubry D, Greaney P, Ireson C, Thougaard AV, et al. The NAD biosynthesis inhibitor APO866 has potent antitumor activity against hematologic malignancies. Blood 2009;113:3276–86.
22. Magni G, Amici A, Emanuelli M, Raffaelli N, Ruggieri S. Enzymology of NAD+ synthesis. Adv Enzymol Relat Areas Mol Biol 1999;73:135–82.
23. Lemke D, Pfenning PN, Sahm F, Klein AC, Kempf T, Warnken U, et al. Costimulatory protein 4IgB7H3 drives the malignant phenotype of glioblastoma by mediating immune escape and invasiveness. Clin Cancer Res 2012;18:105–17.
24. Smythe GA, Poljak A, Bustamante S, Braga O, Maxwell A, Grant R, et al. ECNI GC-MS analysis of picolinic and quinolinic acids and their amides in human plasma, CSF, and brain tissue. Adv Exp Med Biol 2003;527:705–12.
25. Bruna A, Darken RS, Rojo F, Ocana A, Penuelas S, Arias A, et al. High TGF beta-Smad activity confers poor prognosis in glioma patients and promotes cell proliferation depending on the methylation of the PDGF-B gene. Cancer Cell 2007;11:147–60.
26. Toedt G, Barbus S, Wolter M, Felsberg J, Tews B, Blond F, et al. Molecular signatures classify astrocytic gliomas by IDH1 mutation status. Int J Cancer 2011;128:1095–103.
27. Cancer Genome Atlas Research Network. Comprehensive genomic characterization defines human glioblastoma genes and core pathways. Nature 2008;455:1061–8.
28. Gravendeel LA, Kouwenhoven MC, Gevaert O, de Rooi JJ, Stubbs AP, Duijm JE, et al. Intrinsic gene expression profiles of gliomas are a better predictor of survival than histology. Cancer Res 2009;69:9065–72.
29. Roggendorf W, Strupp S, Paulus W. Distribution and characterization of microglia/macrophages in human brain tumors. Acta Neuropathol 1996;92:288–93.
30. Smith DG, Guillemin GJ, Pemberton L, Kerr S, Nath A, Smythe GA, et al. Quinolinic acid is produced by macrophages stimulated by platelet activating factor, Nef and Tat. J Neurovirol 2001;7:56–60.
31. Guillemin GJ, Brew BJ. Microglia, macrophages, perivascular macrophages, and pericytes: a review of function and identification. J Leukoc Biol 2004;75:388–97.
32. Stupp R, Mason WP, van den Bent MJ, Weller M, Fisher B, Taphoorn MJ, et al. Radiotherapy plus concomitant and adjuvant temozolomide for glioblastoma. N Engl J Med 2005;352:987–96.
33. Wick W, Platten M, Meisner C, Felsberg J, Tabatabai G, Simon M, et al. Temozolomide chemotherapy alone versus radiotherapy alone for malignant astrocytoma in the elderly: the NOA-08 randomised, phase 3 trial. Lancet Oncol 2012;13:707–15.
34. Wick W, Platten M, Weller M. New (alternative) temozolomide regimens for the treatment of glioma. Neuro-oncology 2009;11:69–79.
35. Hegi ME, Diserens AC, Gorlia T, Hamou MF, de Tribolet N, Weller M, et al. MGMT gene silencing and benefit from temozolomide in glioblastoma. N Engl J Med 2005;352:997–1003.
36. Felsberg J, Thon N, Eigenbrod S, Hentschel B, Sabel MC, Westphal M, et al. Promoter methylation and expression of MGMT and the DNA mismatch repair genes MLH1, MSH2, MSH6 and PMS2 in paired primary and recurrent glioblastomas. Int J Cancer 2011;129:659–70.
37. Platten M, Kretz A, Naumann U, Aulwurm S, Egashira K, Isenmann S, et al. Monocyte chemoattractant protein-1 increases microglial infiltration and aggressiveness of gliomas. Ann Neurol 2003;54:388–92.
38. Zhai H, Heppner FL, Tsirka SE. Microglia/macrophages promote glioma progression. Glia 2011;59:472–85.
39. Ghosh A, Chaudhuri S. Microglial action in glioma: a boon turns bane. Immunol Lett 2010;131:3–9.
40. Graeber MB, Scheithauer BW, Kreutzberg GW. Microglia in brain tumors. Glia 2002;40:252–9.
41. Munn DH, Sharma MD, Baban B, Harding HP, Zhang Y, Ron D, et al. GCN2 kinase in T cells mediates proliferative arrest and anergy induction in response to indoleamine 2,3-dioxygenase. Immunity 2005;22:633–42.
42. Frumento G, Rotondo R, Tonetti M, Damonte G, Benatti U, Ferrara GB. Tryptophan-derived catabolites are responsible for inhibition of T and natural killer cell proliferation induced by indoleamine 2,3-dioxygenase. J Exp Med 2002;196:459–68.
43. Opitz CA, Wick W, Steinman L, Platten M. Tryptophan degradation in autoimmune diseases. Cell Mol Life Sci 2007;64:2542–63.
44. Ribeiro CA, Grando V, Dutra Filho CS, Wannmacher CM, Wajner M. Evidence that quinolinic acid severely impairs energy metabolism through activation of NMDA receptors in striatum from developing rats. J Neurochem 2006;99:1531–42.
45. Inglis WL, Semba K. Discriminable excitotoxic effects of ibotenic acid, AMPA, NMDA and quinolinic acid in the rat laterodorsal tegmental nucleus. Brain Res 1997;755:17–27.

46. Pawley AC, Flesher S, Boegman RJ, Beninger RJ, Jhamandas KH. Differential action of NMDA antagonists on cholinergic neurotoxicity produced by N-methyl-D-aspartate and quinolinic acid. Br J Pharmacol 1996;117:1059–64.
47. Lehmann J, Schaefer P, Ferkany JW, Coyle JT. Quinolinic acid evokes [3H]acetylcholine release in striatal slices: mediation by NMDA-type excitatory amino acid receptors. Eur J Pharmacol 1983;96:111–5.
48. Grant R, Kapoor V. Inhibition of indoleamine 2,3-dioxygenase activity in IFN-gamma stimulated astroglioma cells decreases intracellular NAD levels. Biochem Pharmacol 2003;66: 1033–6.
49. Grant RS, Passey R, Matanovic G, Smythe G, Kapoor V. Evidence for increased *de novo* synthesis of NAD in immune-activated RAW264.7 macrophages: a self-protective mechanism? Arch Biochem Biophys 1999;372:1–7.
50. Grant RS, Kapoor V. Murine glial cells regenerate NAD, after peroxide-induced depletion, using either nicotinic acid, nicotinamide, or quinolinic acid as substrates. J Neurochem 1998;70: 1759–63.
51. Grant RS, Naif H, Thuruthyil SJ, Nasr N, Littlejohn T, Takikawa O, et al. Induction of indoleamine 2,3-dioxygenase in primary human macrophages by HIV-1. Redox Rep 2000;5: 105–7.
52. Guillemin GJ, Kerr SJ, Smythe GA, Smith DG, Kapoor V, Armati PJ, et al. Kynurenine pathway metabolism in human astrocytes: a paradox for neuronal protection. J Neurochem 2001;78:842–53.
53. Espey MG, Chernyshev ON, Reinhard JF Jr, Namboodiri MA, Colton CA. Activated human microglia produce the excitotoxin quinolinic acid. Neuroreport 1997;8:431–4.
54. Chiarugi A, Calvani M, Meli E, Traggiai E, Moroni F. Synthesis and release of neurotoxic kynurenine metabolites by human monocyte-derived macrophages. J Neuroimmunol 2001;120:190–8.
55. Guillemin GJ, Meininger V, Brew BJ. Implications for the kynurenine pathway and quinolinic acid in amyotrophic lateral sclerosis. Neurodegener Dis 2005;2:166–76.
56. Guillemin GJ, Cullen KM, Lim CK, Smythe GA, Garner B, Kapoor V, et al. Characterization of the kynurenine pathway in human neurons. J Neurosci 2007;27:12884–92.
57. Goellner EM, Grimme B, Brown AR, Lin YC, Wang XH, Sugrue KF, et al. Overcoming temozolomide resistance in glioblastoma via dual inhibition of NAD+ biosynthesis and base excision repair. Cancer Res 2011;71:2308–17.
58. Metzeler KH, Hummel M, Bloomfield CD, Spiekermann K, Braess J, Sauerland MC, et al. An 86-probe-set gene-expression signature predicts survival in cytogenetically normal acute myeloid leukemia. Blood 2008;112:4193–201.